

Contents lists available at [ScienceDirect](http://ScienceDirect.com)

## Materials Science and Engineering C

journal homepage: [www.elsevier.com/locate/msec](http://www.elsevier.com/locate/msec)

## Silver activation on thin films of Ag–ZrCN coatings for antimicrobial activity

I. Ferreri<sup>a,b,\*</sup>, S. Calderon V.<sup>a,c</sup>, R. Escobar Galindo<sup>d</sup>, C. Palacio<sup>e</sup>, M. Henriques<sup>b</sup>, A.P. Piedade<sup>c</sup>, S. Carvalho<sup>a,c</sup><sup>a</sup> GRF-CFUM, University of Minho, Campus of Azurém, 4800-058 Guimarães, Portugal<sup>b</sup> CEB, Centre for Biological Engineering, LIBRO-Laboratório de Investigação em Biofilmes Rosário Oliveira, University of Minho, Campus of Gualtar, 4700-057 Braga, Portugal<sup>c</sup> CEMUC, Mechanical Engineering Department, University of Coimbra, 3030-788 Coimbra, Portugal<sup>d</sup> Instituto de Ciencia de Materiales de Madrid (ICMM–CSIC), Cantoblanco, 28049 Madrid, Spain<sup>e</sup> Departamento de Física Aplicada, Universidad Autónoma de Madrid, 28049 Madrid, Spain

## ARTICLE INFO

## Article history:

Received 13 October 2014

Received in revised form 17 April 2015

Accepted 28 May 2015

Available online 3 June 2015

## Keywords:

Sputtering

Biomaterial

Bacterial adhesion

Silver activation

## ABSTRACT

Nowadays, with the increase of elderly population and related health problems, knee and hip joint prosthesis are being widely used worldwide. However, failure of these invasive devices occurs in a high percentage thus demanding the revision of the surgical procedure. Within the reasons of failure, microbial infections, either hospital or subsequently-acquired, contribute in high number to the statistics. *Staphylococcus epidermidis* (*S. epidermidis*) has emerged as one of the major nosocomial pathogens associated with these infections. Silver has a historic performance in medicine due to its potent antimicrobial activity, with a broad-spectrum on the activity of different types of microorganisms. Consequently, the main goal of this work was to produce Ag–ZrCN coatings with antimicrobial activity, for the surface modification of hip prostheses.

Thin films of ZrCN with several silver concentrations were deposited onto stainless steel 316 L, by DC reactive magnetron sputtering, using two targets, Zr and Zr with silver pellets (Zr + Ag target), in an atmosphere containing Ar, C<sub>2</sub>H<sub>2</sub> and N<sub>2</sub>. The antimicrobial activity of the modified surfaces was tested against *S. epidermidis* and the influence of an activation step of silver was assessed by testing samples after immersion in a 5% (w/v) NaClO solution for 5 min.

The activation procedure revealed to be essential for the antimicrobial activity, as observed by the presence of an inhibition halo on the surface with 11 at.% of Ag. The morphology analysis of the surface before and after the activation procedure revealed differences in silver distribution indicating segregation/diffusion of the metallic element to the film's surface.

Thus, the results indicate that the silver activation step is responsible for an antimicrobial effect of the coatings, due to silver oxidation and silver ion release.

© 2015 Elsevier B.V. All rights reserved.

## 1. Introduction

With the increase of the elderly population and health problems, that are arising nowadays, the number of hip joint prosthesis used worldwide is rapidly growing, and is unfortunately associated with a rising number of implant-associated infections [1,2]. Bacterial adhesion on implants is the initial cause of infection [3], and can be translated to the serious risk of implants' failure, with all negative consequences for the patient, health services and the high costs associated [4]. Even with all surgical procedures, like medical devices sterilization and skin preparation [5], bacterial infection at the site of implanted medical

devices, such as catheters and artificial prosthetics, presents a serious problem in the biomedical field [2,6–8].

Implant infections in orthopedics, as well as in many other medical fields, are mainly caused by staphylococci [9]. *Staphylococcus epidermidis* (*S. epidermidis*) has emerged as one of the major nosocomial pathogens associated with these infections. This bacterium is an opportunistic microorganism and has the ability to resist to antibiotic therapy and host defenses [10], which may explain the significant number of implant-associated infections. The initial adhesion of these microorganisms to biomaterials' surface is thought to be an important stage in their colonization [11]. The infectious pathogens are motionless, or metabolically inactive, during the first six hours after surgery, period known to be critical for preventing infection [12]. Thereafter, bacterial biofilm – defined as a structured community of bacterial cells enclosed in a self-produced polymeric matrix and that are adherent to an inert or living surface [4] – is often associated with these types of infections. Once the bacterial community is in the biofilm stage antibiotic treatments do not reveal efficacy, and

\* Corresponding author at: GRF-CFUM, University of Minho, Campus of Azurém, 4800-058 Guimarães, Portugal.

E-mail address: [isabelferreri@gmail.com](mailto:isabelferreri@gmail.com) (I. Ferreri).

the growing antibiotic resistance of pathogenic bacterial species is a serious problem for public health [13]. For these reasons, it is better to prevent the earlier stages of bacteria adhesion, instead of trying to eliminate the problem at a later phase where microorganisms are in a more complex stage, which demands new approaches in the orthopedic field, in order to reduce patient morbidity and mortality associated to hip surgery infection [14], and consequently reduce health costs [6].

One of the strategies is the modification of implant surfaces [7,15,16] with the aim of eliminating the infection of biomedical implants [6,17], and also improving their chemical, mechanical, and tribological characteristics, important features in biomedical devices. The use of nanocomposite protective films, based on the combination of various transition metal carbides, nitrides and carbonitrides, has already been reported [18–23]. Within these materials, zirconium carbonitride (ZrCN) starts to appear as a promising material for biomedical use [24–26].

Silver has a historic performance in medicine due to its powerful antimicrobial activity [27–34], with a broad-spectrum of activity against different microorganisms which usually implies the oxidation of metallic silver to  $\text{Ag}^+$  [35,36]. Since bacterial infections are associated with prosthetic failures, silver has been considered as a coating of invasive medical devices [37], not only due to its reported antimicrobial effect but also because due to the absence of toxicity of the active  $\text{Ag}^+$  to human cells [36].

Although the mechanism of silver antimicrobial activity is not fully understood, it is suggested that silver ions act by strongly binding to critical biological molecules (proteins, DNA, RNA), disrupting their functions [30,35], as well as by generating reactive oxygen species (ROS), which are toxic to bacterial cells, obtaining a synergic bactericidal effect between ionic silver and ROS [38]. However, in a recent study published by Carvalho et al. [39], using Ag–TiCN system, silver ionization seems to be insufficient or even non-existent and the samples did not show antimicrobial activity. So, in order to promote antimicrobial activity, on this type of coatings, it is essential that the silver ionization occurs, preventing microbial adhesion and subsequent biofilm formation. Therefore, the proposed challenge for this type of materials is to ensure the ionization of silver, since metallic silver present in the coatings is not an active chemical element and has a very low rate of dissolution in biological media [40].

This work reports the deposition of metallic silver (11 atomic percent (at.%) embedded in a zirconium carbonitride (ZrCN) matrix onto stainless steel 316 L substrates, by DC reactive magnetron sputtering. This multiphase structure may have effect on the biological properties of the coatings [41], also reported by other studies [42]. Thereafter, coatings were subjected to a treatment with 5% (w/v) sodium hypochlorite ( $\text{NaClO}$ ), designed as silver activation, in order to increase the rate of silver oxidation.  $\text{NaClO}$  is known as a sterilizing agent in many different fields, such as water purification, metal disinfection and the sterilization of wounds [43].

In this paper the silver activation process to enhance the antibacterial properties of Ag–ZrCN coatings is reported. The morphological and chemical changes before and after the activation procedure were monitored to assess the antimicrobial activity of the developed surfaces.

## 2. Materials and methods

### 2.1. Coatings production

The coatings were deposited onto 316 L stainless steel substrates by unbalanced magnetron sputtering in a closed field configuration known as Physical Vapor Deposition (PVD) process. Prior to each deposit, a cleaning pre-treatment was performed, on the substrates, to remove all impurities and traces of grease, by ultrasonic baths using distilled water after ethanol and then acetone during 10 min for each solution. The two targets (one of pure zirconium and another composed by zirconium and silver pellets) and substrates were further cleaned by an in-situ argon plasma etching process, during 20 min, to eliminate

remaining impurities on the surfaces. After the cleaning process, a zirconium interlayer was deposited, in order to ensure good adhesion between the stainless steel and Ag–ZrCN multifunctional coating. Finally, the coatings were produced using a pure Zr target and a modified Zr target with silver pellets placed on the erosion area (Zr–Ag target). The current density of  $10 \text{ mA cm}^{-2}$  was kept constant for the Zr target, but the current density of the Zr–Ag target was changed between 0 and  $2.5 \text{ mA cm}^{-2}$ . With these conditions, two samples were produced, one without silver, named Ag 0, and another with 11 at.% of silver, named Ag 11. To obtain homogenous multifunctional Ag–ZrCN coatings, samples were placed on a rotational substrate holder at a constant speed of 8 rpm. The sputtering atmosphere was kept in a constant flow of argon (60 standard cubic centimeters per minute (sccm)), acetylene (1.2 sccm) and nitrogen (4 sccm). The deposition temperature (373 K), polarization potential on the substrate holder (bias) ( $-50 \text{ V}$ ), and work pressure ( $2.1 \times 10^{-1} \text{ Pa}$ ) were monitored and kept constant during the deposition.

### 2.2. Silver activation

All samples used in this study were sterilized by autoclave, for 15 min, at  $121^\circ \text{C}$ . In order to improve the oxidation of silver, an activation procedure was performed by immersing the samples in a 5% (w/v) commercial sodium hypochlorite ( $\text{NaClO}$ ) solution (Limpolar, Portugal) for 5 min. After three consecutive washes in deionized water, to remove the remaining oxidizing solution, samples were dried on air (inside a flow chamber) and tested. The activation procedure was also performed on zirconium carbonitride coatings without silver (Ag 0), to control the process and verify possible degradation of the coating when immersed in the oxidant.

The morphology of each coating (before and after activation) was evaluated by Scanning Electron Microscopy (NanoSEM 200-EDAX-Nova) in both backscattering (BSE) and secondary electron (SE) modes.

### 2.3. Chemical and physical analysis

The chemical composition of the coatings, as-deposited, was determined by electron probe microanalysis technique (EPMA) using a Cameca equipment, model Camebax SX50. Five measurements were performed for each sample on randomly selected zones of the surface. The accelerating voltage of the electron beam was 10 kV and the current 40 nA.

The evolution of the compositional profile of the coatings before and after activation was evaluated by Glow Discharge Optical Emission Spectroscopy (GDOES). GDOES experiments were performed to assess the compositional profile of the sterilized as deposited Ag–ZrCN coatings (Ag 11), Ag 11 coatings after the activation process (Ag 11\_act) and Ag 11\_act coatings after the microbiological halo test (Ag 11\_act after Halo). GDOES experiments were also performed on ZrCN coatings, before (Ag 0) and after activation (Ag 0\_act). The tests were performed using a Jobin Yvon RF GD Profiler equipped with a 4 mm diameter anode and operating at a typical radio frequency discharge pressure of 650 Pa and a power of 40 W.

X-ray photoelectron spectroscopy (XPS) was used for the characterization of the oxidation states of the chemical elements of the coating before and after the activation step as well as after the microbiological tests. XPS spectra were acquired in an ultrahigh vacuum system at a base pressure below  $8 \times 10^{-8} \text{ Pa}$  using a hemispherical analyzer (SPECS EA-10 Plus). The pass energy was 15 eV giving a constant resolution of 0.9 eV. The Ag 3d<sub>5/2</sub> line at 367.9 eV was used in order to calibrate the binding energies. A twin anode (Mg and Al) x-ray source was operated at a constant power of 300 W using Mg K $\alpha$  radiation. The samples were not sputter-cleaned. Deconvolution software CasaXPS was used for spectra analysis of the samples.

## 2.4. Antimicrobial properties

The antibacterial activity of Ag–ZrCN coatings was examined using the zone of inhibition (ZOI) test [29], using the size of the growth inhibition halo as a qualitative measure of the activity of the sample.

In preparation for the ZOI study assays, a single colony of *S. epidermidis* (*S. epidermidis*, IE186 strain, a clinical isolate belonging to the CEB Biofilm Group collection) was inoculated on Tryptic Soy Broth (TSB, Merck) and incubated for 18 h at 37 °C, and 120 rpm. Thereafter, the resultant cell suspension was adjusted to an optical density (OD) of 1.0 at 640 nm, measured on ELISA (enzyme-linked immunosorbent assay) absorbance reader (Sunrise™, Tecan, Austria) and properly diluted to obtain  $1 \times 10^7$  CFU · mL<sup>-1</sup>.

1 mL of the cellular suspension was added to 14 mL of cooled TSA agar (TSA, Merck) and after placed into sterile plastic Petri dishes. After agar medium solidification, the sterilized Ag–ZrCN samples (before and after activation) were placed on the center of the Petri dishes and cultured for 24 h, at 37 °C. Following the incubation period, the zone of transparent medium formed around the sample was measured, indicative of bacteria growth absence. All experiments were run in triplicate per sample (technical replicates), on three independent occasions (biological replicates).

## 3. Results and discussion

In this work, coatings deposited by reactive magnetron sputtering were submitted to an activation procedure in order to evaluate its effect on the enhancement of silver ionization. The modified surfaces were characterized by several techniques and their antimicrobial activity estimated.

### 3.1. Chemical and physical analysis

Table 1 shows the chemical composition of the samples as-deposited, measured by EPMA. Further details concerning the chemical composition versus deposition parameters, of the similar samples, can be found elsewhere [44,45].

The films' morphology was evaluated before and after the activation process, to verify the existence of morphological alterations and/or film delamination due to the oxidizing agent activity. Fig. 1a) shows the Ag 0 coatings before activation, revealing pronounced boundaries mimicking the substrate grains and a characteristic columnar structure (inset in Fig. 1a)). After the activation process (Fig. 1b)), the coatings morphology did not change significantly and no evidence of film delamination was observed. In fact, other researchers have reported that ZrCN coatings are resistant to hydrogen peroxide (H<sub>2</sub>O<sub>2</sub>), an oxidizing agent used in hospital environment [24].

Ag 11 coatings exhibit an overall morphology similar to coatings before silver activation, Ag 0 (Fig. 2a)), but with silver nanoparticles distributed on the surface. After the activation procedure (Fig. 2b)), significant morphological changes were noted, showing the formation of silver-based nanoparticles dispersed over the entire film surface. These results suggest that the NaClO solution penetrates the coating,

thus activating not only the superficial silver but also some silver present within the coating, leading to changes in surface morphology. Nevertheless, it is also important to understand the distribution of silver along the coating thickness and how deep the oxidizing agent evolve within the coatings, in order to promote silver ionization and its subsequent migration to the coating surface. Hence, for further investigation of Ag diffusion through the coating and evolution in terms of distribution, a GDOES technique was performed.

Figs. 3 and 4 show the GDOES depth profile composition of the sample Ag 11 before and after activation, respectively, revealing very different silver distribution profiles mainly on the surface of the film, confirming the observations made by SEM (Fig. 2). In fact, a significant increase in the silver concentration is visible for the first 7 nm in the activated samples (Fig. 4), that should be promoted from silver segregation/diffusion from the inside to the film surface. This behavior was not observed before activation, being reported for similar materials only after thermal annealing [46]. The other chemical elemental composition did not vary significantly, confirming the stability of the ZrCN phase after the activation process.

The results presented in Fig. 4 corroborate the fact that silver activation process can induce the oxidation of silver promoting the diffusion of the metallic ion through the coating, increasing the concentration of silver on the surface, without compromising the overall chemical composition integrity. This diffusion/segregation and the chemical reaction between silver and the oxidant agent, is achieved during few minutes of the activation process, which contributes to the protection of the coating of possible oxidative attacks. Despite the surface changes, it is important to highlight the fact that only the first 7 nm of the film surface is modified which may also be related to the short time of the activation step and to the dense morphology presented by the Ag 11 coating (Fig. 2a)).

### 3.2. XPS analysis

SEM and GDOES results indicate that the major changes occurred at the surface of the coatings and therefore XPS technique was used to characterize the oxidation state of the major chemical elements. It is worth noting that coatings were not sputtered before analysis, leading to the presence of all environmental contaminants, thereby ensuring that key elements present on the surface of the samples would not be disposed of as contaminants.

The binding energy results are shown in Fig. 5. For the Ag 11 and Ag 11\_act surfaces, the C–C bond, at 285.0 eV [47], indicate the presence of an amorphous carbon phase, characteristic of these films [22,44,45,48]. The C 1 s high resolution spectra also shows peaks at ~286.4 and ~288.1 eV, attributed either to C–N and C–O bonds, which could indicate both CN<sub>x</sub> amorphous phases [49]. This fact correlates with the component observed at ~399 eV in the N 1 s, for Ag 11.

The results of Ag 11 as-deposited show the Zr–O bond (182.3 eV) [22], revealing the high reactivity of this element with the environment and its ability to form passive layers, that could benefit the corrosion resistance [48], important features for biomedical devices. After the activation procedure, it is believed that this passive ZrO<sub>2</sub> layer remains on the material surface, in its hydrated form, which explains the decrease of its binding energy [50]. However, the main focus is on the silver spectrum for the different surfaces: Ag 11 and Ag 11\_act. For Ag 11 the silver spectra revealed a broad band at 369.4 eV, in addition to the metallic peak at 368.4 eV. The former band is attributed to metallic sub-nanoparticles associated with clusters smaller than 4 nm [51]. This band has also been observed by Calderon et al. [44] in ZrCN–Ag samples. After the activation procedure, the peaks related to Ag-clusters and metallic silver disappear and a new peak arises, shifted to lower energies, which can be attributed to silver oxides, since oxidation leads to shifting of binding energy to lower values accompanied by a peak broadening, which clearly discloses the oxidation of silver to Ag<sup>+</sup> state [52]. In fact, the silver oxide peak was identified at 367.8 eV, confirming the surface

**Table 1**

Chemical composition of the deposited coatings, measured by EPMA (with standard deviation between 0.2 and 0.8) and current density applied to each target, during the deposition.

Samples	Coating composition (at. %)					J <sub>Zr</sub> (mA/cm <sup>2</sup> )	J <sub>Zr + Ag</sub> (mA/cm <sup>2</sup> )
	Zr	N	C	O	Ag		
Ag 0	36	19	37	8	0	10	0
Ag 11	32	29	19	9	11	7.5	2.5

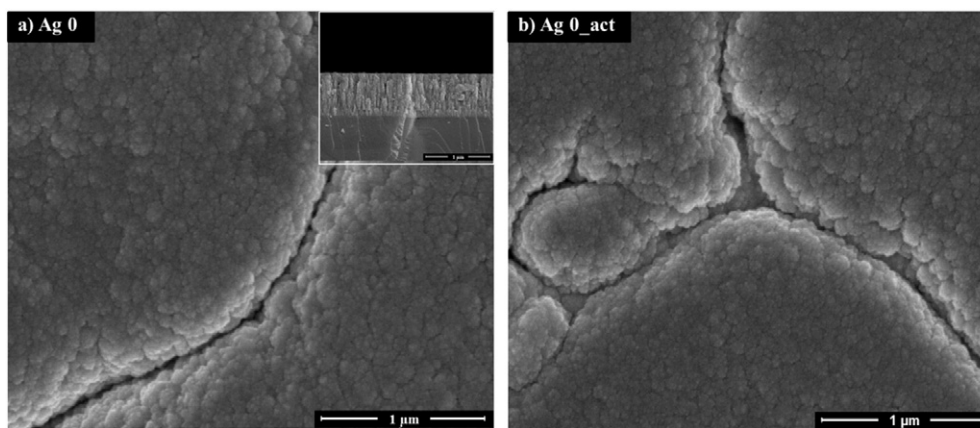


Fig. 1. SEM micrographs of the surface of the Ag 0 thin film: a) before and b) after activation with NaClO. The inset in a) presents the Ag 0 samples cross-section view.

silver oxidation during the activation process. Due to the small size and intrinsic characteristics, clusters in coatings are more easily ionized. When the coatings are immersed in the sodium hypochlorite, the solution penetrates into the coating, oxidizes the silver, with subsequent diffusion of ions to the surface, where returns to the oxide compound once the surface is removed from the solution. This explains the emergence of this new peak and the absence of the clusters and metallic peaks. These findings are in agreement with the peak observed at 529.7 eV, in the O 1 s high resolution spectra, with evident changes before and after activation.

There is no evidence of chloride in the samples after the activation procedure, which can be considered contradictory to the well-known affinity of silver to chlorinated solutions [53], inducing the formation of AgCl. Thus, more insights are needed, in the reaction mechanism on silver activation, in order to understand the chemical reaction between silver in the coatings and the oxidant agent.

### 3.3. Mechanism on silver activation

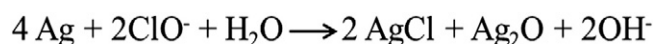
It is well known that the antimicrobial activity of silver is dependent of the presence of silver ions. The  $\text{Ag}^+$  easily binds to electron donor groups from biological molecules containing sulfur (S), oxygen (O) or nitrogen (N), also leading to the formation of reactive oxygen species (ROS), which are toxic to bacterial cells [54]. Thus, for an effective

antimicrobial effect, the formation and release of ionic silver to the pathogenic medium is required [36].

To promote the active and powerful silver ionization, an activation procedure was performed using an oxidizing compound, as described in Section 2.

The reaction between metallic silver (presented in the Ag 11 coatings) and the sodium hypochlorite, named silver activation, is presented in Scheme 1.

Scheme 1. Chemical reaction between silver and sodium hypochlorite



Scheme 1.

Due to the large affinity between silver and chloride solutions [53], together with the enthalpy of formation of AgCl ( $\Delta_f H_{298}^\circ = -127.01 \text{ kJ mol}^{-1}$ ), which is more negative than  $\text{Ag}_2\text{O}$  ( $\Delta_f H_{298}^\circ = -31.1 \text{ kJ mol}^{-1}$ ) [55], it was expected that this reaction produces a majority of silver chloride (AgCl). However, we hypothesized that when in contact with the aqueous hypochlorite solution, an alkaline and strong oxidant medium, silver in the Ag-ZrCN coatings may firstly form AgOH on its surface. While AgOH is not stable at room temperature, his enthalpy of formation ( $\Delta_f H_{298}^\circ = -125.7 \text{ kJ mol}^{-1}$ ) is very similar to AgCl ( $\Delta_f H_{298}^\circ = -127.01 \text{ kJ mol}^{-1}$ ), serving as a measure of the

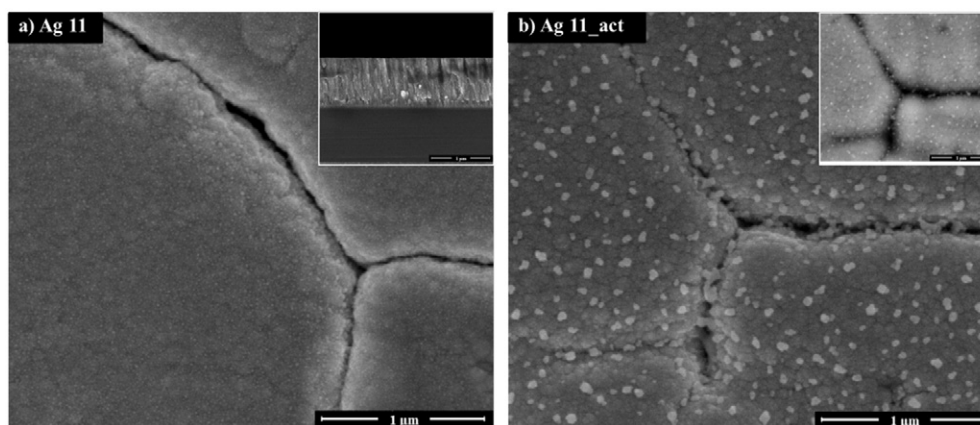


Fig. 2. SEM micrograph of the surface of the Ag 11 thin film: a) before and b) after activation with NaClO. The inset in a) presents the Ag 11 samples cross-section view and the inset in b) show the SEM image from the sample surface where Ag agglomerates (BSE image) is evident.

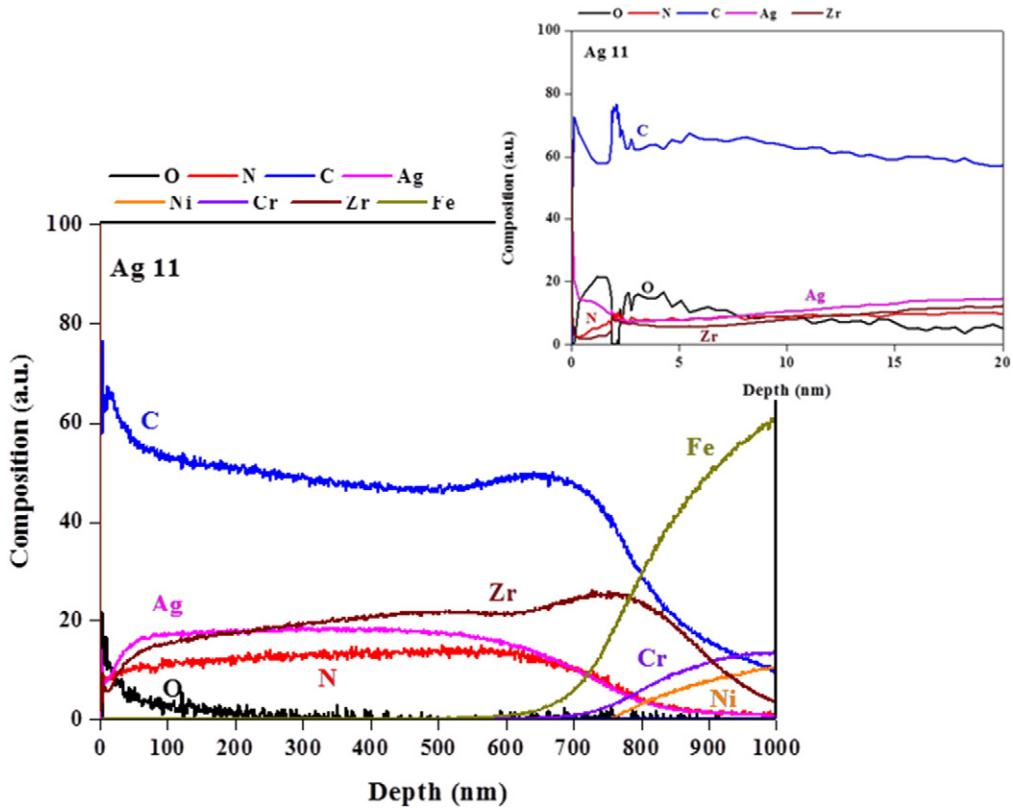


Fig. 3. GDOES profile of Ag 11 thin film, before activation with NaClO. The inset in the figure shows the profile in the first 20 nm of the coating.

relative bond strengths [56]. Silver oxidation is preceded by adsorption of hydroxyl ions, whose presence has been proved on silver electrode surface [57]. Hence, during the activation procedure, a competitive

adsorption of  $\text{OH}^-$  and  $\text{Cl}^-$  on silver surface may explain the preferential formation of silver hydroxide instead of silver chloride. Subsequently, silver hydroxide will induce the formation of  $\text{Ag}^+$  according to

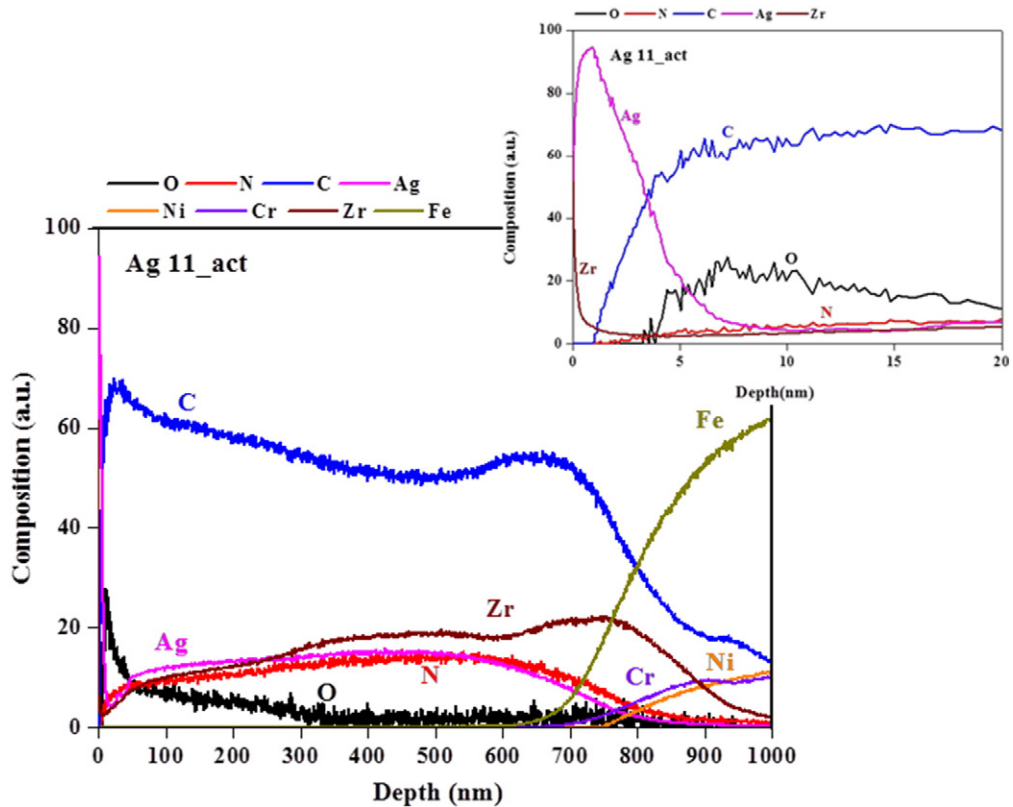


Fig. 4. GDOES profile of Ag 11 thin film after activation with NaClO. The inset in the figure shows the profile in the first 20 nm of the coating.

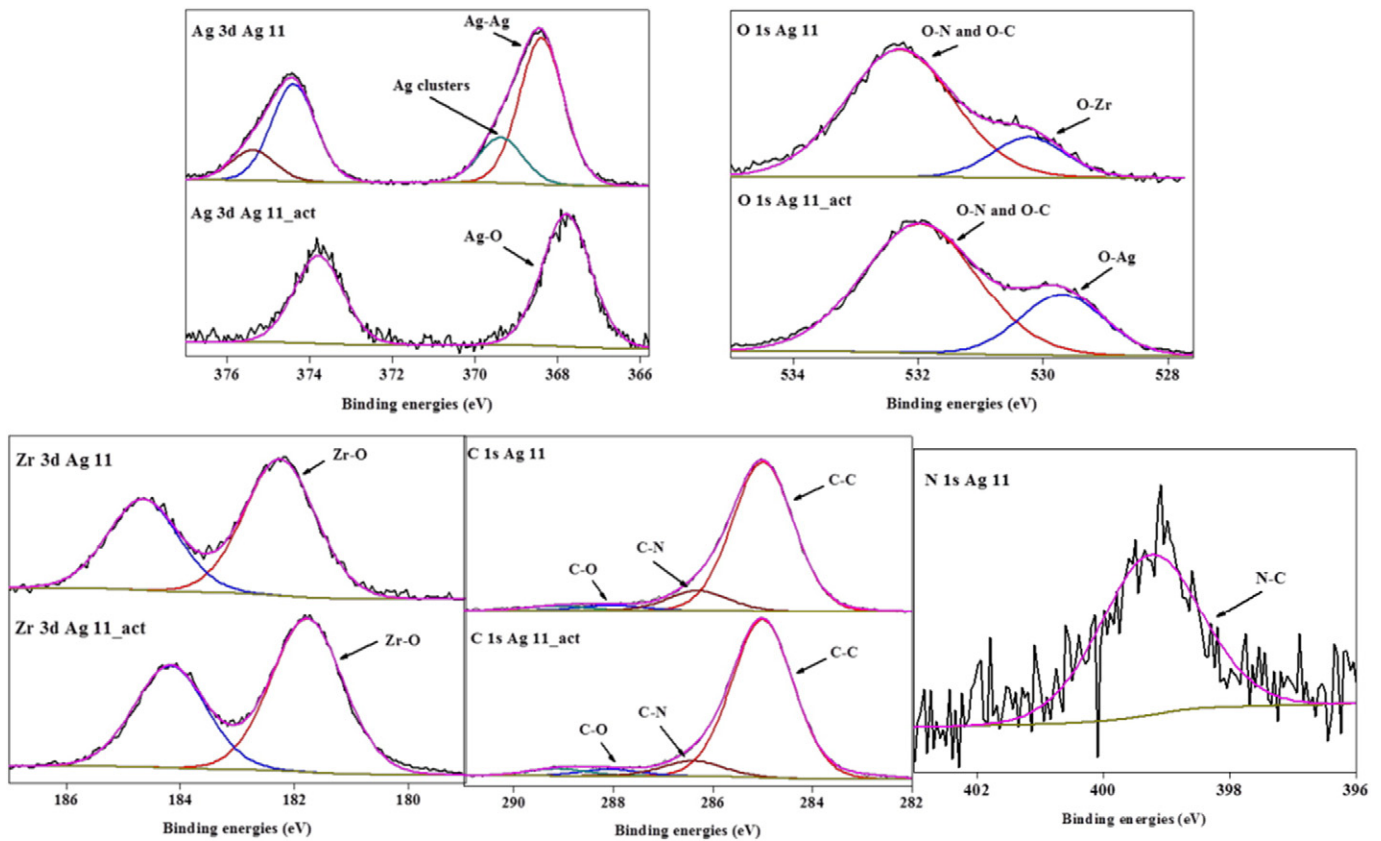
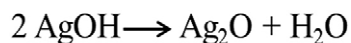


Fig. 5. XPS spectra of Ag 3d, O1s, Zr 3d C1s and N1s core levels of the Ag 11 and Ag 11\_act coatings.

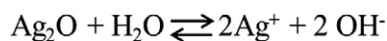
Schemes 2 and 3. These results are in agreement with XPS analysis where Ag–O is identified in the coating surface after the activation procedure and no evidences of the Ag–Cl bond were detected.

Scheme 2. Silver oxide formation from silver hydroxide



Scheme 2.

Scheme 3. Formation of  $\text{Ag}^+$  from silver oxide



Scheme 3.

In fact, the formation of oxidized nano silver was the focal point in this procedure, which can inhibit bacterial growth [53], since its bio-availability allows increasing biocidal  $\text{Ag}^+$  formation and mobility, providing a constant concentration of  $\text{Ag}^+$  ions in aqueous environments [40].

In order to demonstrate the release of  $\text{Ag}^+$  into the biological medium and subsequently the antimicrobial activity of these activated silver coatings, antimicrobial tests were performed.

### 3.4. Antimicrobial properties

Fig. 6 shows the growth inhibition halo tests performed using Ag 11 coatings, before (a) and after (b) silver activation, as well as Ag 0 coating after activation (c). The pathogenic bacteria and medium selected for

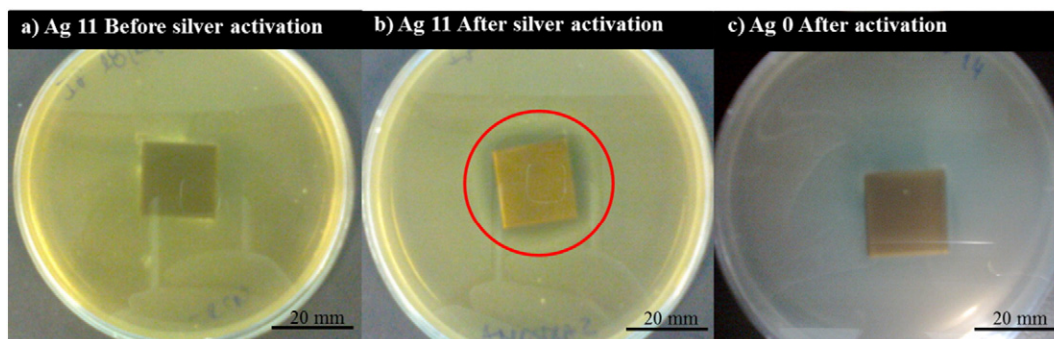


Fig. 6. Growth inhibition halo tests: a) Ag 11 coating with no halo, b) Ag 11\_act coating, after silver activation, with red circle highlighting the formation of the growth inhibition halo, and c) Ag 0 after activation with no antimicrobial activity.

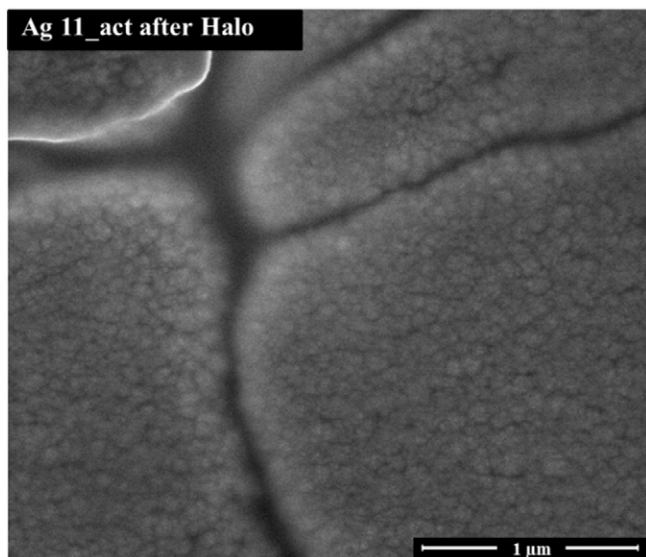


Fig. 7. SEM micrograph of the surface of the activated Ag 11 thin film after the microbiological test.

these assays, closely mimic real conditions of biomedical implants' colonization [40].

From Fig. 6, it is clear that the growth inhibition halo (clear biological medium, with no bacteria growth) formed around the sample after activation (Fig. 6b)), an indicator of antimicrobial activity. These results can be explained considering the chemical reaction which takes place during the activation procedure. During the activation process, silver oxide was formed on surface, as previously discussed.  $\text{Ag}^+$  was formed (Scheme 3) when in close contact with a moist and electrolyte medium, and spontaneously diffuses to the surrounding medium (bacteria suspension and agar), killing or inhibiting bacteria growth [15]. Antimicrobial activity in Ag 11 activated coating was noticed during the 24 h of the halo test. According to Poelstra and Barekzi [12], the first 6 h after surgery is crucial for

preventing infection, since the infectious pathogens are still latent or metabolically inactive. During the first 24 h of colonization and contact between bacteria and the indwelling medical devices, biofilm develops and becomes mature [3], indicating that microorganisms are irreversibly attach and enclosed in a matrix of exopolymeric products [4], resisting to the host immune system and antibiotic treatment.

In the entire process, Ag 0 coatings were used as control before and after immersion on  $\text{NaClO}$ , to eliminate the possibility that the oxidizing agent residues could be responsible for bacteria death. No growth inhibition zone was observed for both Ag 0 and Ag 0\_act, excluding the action of the remaining oxidizing agent. Also no bacterial inhibition growth was seen on sterilized as-deposited Ag 11 coating (Fig. 6a)).

SEM, GDOES assay and XPS spectroscopy were also performed on activated coating, Ag 11, after contact with the microbiological test (Ag 11\_act after halo). Remarkably, SEM analysis reveals that there are no visible silver-based nanoparticles on the coating surface (Fig. 7), in agreement with the composition analysis made by GDOES and XPS, as shown in Figs. 4 and 5. The silver of the surface layer of Ag 11\_act disappeared after contact with the biological medium of the microbiological test (Ag 11\_act after halo), which indicates that during the incubation period silver ionizes and subsequently diffuses through the culture medium, suppressing the functions of microbial cells, leading to their death. This fact is further confirmed by XPS results, where is possible to observe the decrease of silver concentration (Fig. 8 inset).

Due to the stability of the ZrCN matrix it is desirable that silver is located close to the surface, since bacterial adhesion and proliferation take place on the surface of the material [6]. Previously to the activation step, as mentioned, silver nanoparticles were embedded in the ZrCN coating, visible but less available to ionize and react with the surrounding environment. After the activation procedure, significant changes in shape, size, distribution density of the silver particles and cover ratio have been achieved, as discussed on basis of SEM micrographs (Fig. 2), GDOES profile (Fig. 4) and XPS spectra (Fig. 5). The silver based nanoparticles have diffused to the surface of Ag 11 coating, increasing its availability to ionize and diffuse through the biological medium during the growth inhibition halo test. These nanoparticles are in fact strongly attached to the matrix since they are not removed by mechanical manipulation of the samples and successive washings performed before

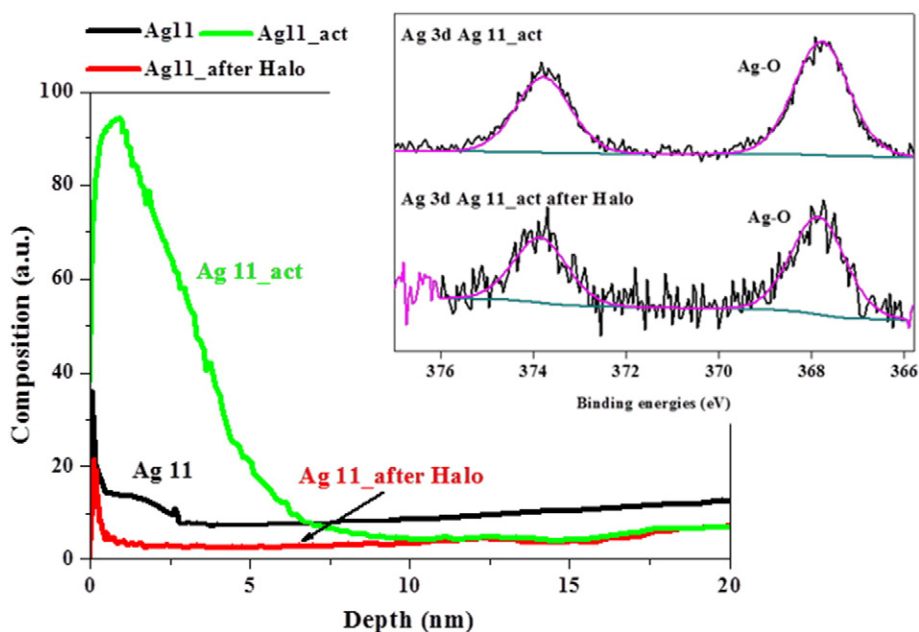


Fig. 8. GDOES silver profile of different coatings: Ag 11 (as-deposited), Ag 11\_act (activated) and Ag 11\_act after halo (after growth inhibition halo test), in the first 20 nm. The inset represents the silver XPS profile in the Ag 11\_act and Ag 11\_act after halo test (coatings before and after halo test).

the microbiological test. This binding mechanism and its relation with antimicrobial activity is not yet fully investigated and understood. However, it is clear that after exposure to the culture medium, silver ion release occurs in the activated Ag 11 coating, granting the antimicrobial activity observed (Fig. 6).

The results show the abrupt decrease of silver content on the outermost layer after the microbiological tests in agreement with SEM observation (Fig. 7), probably due to silver diffusion into the culture medium, in contrast with the profile of the activated coating, where a high silver concentration can be observed in the first 7 nm (Fig. 4).

#### 4. Conclusion

In order to increment the silver ionization in samples with approximately 11% of Ag, sample Ag 11, a silver activation procedure, with 5% (w/v) NaClO solution, was successfully performed. This method induced significant changes in shape, size and distribution density of the silver particles, as well as an increase of the cover ratio. XPS results disclosed the presence of silver oxides on the coatings surface, after NaClO immersion. This activated Ag 11 coating showed an antimicrobial effect, according to the growing inhibition halo test, suggesting that silver ions diffuse through the media.

SEM images obtained after the microbiological tests revealed an enormous decrease in silver content, showing the silver top layer disappearance.

The results demonstrate that the developed Ag–ZrCN coatings, after the activation process, have potential to reduce bacteria adhesion and consequently biofilm formation on medical devices.

#### Acknowledgments

IF acknowledges the financial support of FCT—Fundação para a Ciência e a Tecnologia through grant SFRH/BD/71139/2010.

This research is partially sponsored by FEDER funds through the program COMPETE—Programa Operacional Factores de Competitividade and by Portuguese national funds through FCT—Fundação para a Ciência e a Tecnologia, under the projects ANTIMICROBOAT—PTDC/CTM/102853/2008 and in the framework of the Strategic Projects PEST-C/FIS/UI607/2011, and PEST-C/EME/UI0285/2011.

The authors thank the FCT Strategic Project PEST-OE/EQB/LA0023/2013 and the Project “BioHealth—Biotechnology and Bioengineering approaches to improve health quality”, Ref. NORTE-07-0124-FEDER-000027, co-funded by the Programa Operacional Regional do Norte (ON.2 — O Novo Norte), QREN, FEDER. The authors also acknowledge the project “Consolidating Research Expertise and Resources on Cellular and Molecular Biotechnology at CEB/IBB”, Ref. FCOMP-01-0124-FEDER-027462.

#### References

- [1] L. Bernard, P. Hoffmeyer, M. Assal, P. Vaudaux, J. Schrenzel, D. Lew, Trends in the treatment of orthopaedic prosthetic infections, *J. Antimicrob. Chemother.* 53 (2004) 127–129.
- [2] E.M. Hetrick, M.H. Schoenfisch, Reducing implant-related infections: active release strategies, *Chem. Soc. Rev.* 35 (2006) 780–789.
- [3] G. Zhao, L. Ye, Y. Huang, D. Yang, L. Li, G. Xu, et al., In vitro model of bacterial biofilm formation on polyvinyl chloride biomaterial, *Cell Biochem. Biophys.* 61 (2011) 371–376.
- [4] J.W. Costerton, P.S. Stewart, E.P. Greenberg, Bacterial biofilms: a common cause of persistent infections, *Science* 284 (80-) (1999) 1318–1322.
- [5] J. Hades, H. Ahrens, C. Gebert, A. Streitburger, H. Buerger, M. Erren, et al., Lack of toxicological side-effects in silver-coated megaprotheses in humans, *Biomaterials* 28 (2007) 2869–2875.
- [6] M.L.W. Knetsch, L.H. Koole, New strategies in the development of antimicrobial coatings: the example of increasing usage of silver and silver nanoparticles, *Polymers (Basel, Switz.)* 3 (2011) 340–366.
- [7] J. Zhao, H.J. Feng, H.Q. Tang, J.H. Zheng, Bactericidal properties of silver implanted pyrolytic carbon, *Nucl. Instrum. Methods Phys. Res., Sect. B* 243 (2006) 299–303.
- [8] M. Roy, G. a Fielding, H. Beyenal, A. Bandyopadhyay, S. Bose, Mechanical, in vitro antimicrobial, and biological properties of plasma-sprayed silver-doped hydroxyapatite coating, *ACS Appl. Mater. Interfaces* 4 (2012) 1341–1349.
- [9] C.R. Arciola, D. Campoccia, P. Speziale, L. Montanaro, J.W. Costerton, Biofilm formation in Staphylococcus implant infections. A review of molecular mechanisms and implications for biofilm-resistant materials, *Biomaterials* 33 (2012) 5967–5982.
- [10] B.J. Nablo, A.R. Rothrock, M.H. Schoenfisch, Nitric oxide-releasing sol-gels as antibacterial coatings for orthopedic implants, *Biomaterials* 26 (2005) 917–924.
- [11] N. Cerca, G.B. Pier, M. Vilanova, R. Oliveira, J. Azeredo, Quantitative analysis of adhesion and biofilm formation on hydrophilic and hydrophobic surfaces of clinical isolates of Staphylococcus epidermidis, *Res. Microbiol.* 156 (2005) 506–514.
- [12] K. Poelstra, N. Barekzi, Prophylactic treatment of gram-positive and gram-negative abdominal implant infections using locally delivered polyclonal antibodies, *J. Biomed. Mater. Res.* 60 (2002) 206–215.
- [13] A. Kurek, A.M. Grudniak, A. Krackiewicz-Dowjat, K.I. Wolska, New antibacterial therapeutics and strategies, *Pol. J. Microbiol.* 60 (2011) 3–12.
- [14] B. Li, X. Liu, C. Cao, F. Meng, Y. Dong, T. Cui, et al., Preparation and antibacterial effect of plasma sprayed wollastonite coatings loading silver, *Appl. Surf. Sci.* 255 (2008) 452–454.
- [15] L. Chen, L. Zheng, Y. Lv, H. Liu, G. Wang, N. Ren, et al., Chemical assembly of silver nanoparticles on stainless steel for antimicrobial applications, *Surf. Coat. Technol.* 204 (2010) 3871–3875.
- [16] C.J. Chung, H.I. Lin, J.L. He, Antimicrobial efficacy of photocatalytic TiO<sub>2</sub> coatings prepared by arc ion plating, *Surf. Coat. Technol.* 202 (2007) 1302–1307.
- [17] C. Vuong, M. Otto, Staphylococcus epidermidis infections, *Microbes Infect.* 4 (2002) 481–489.
- [18] S. Carvalho, L. Rebouta, E. Ribeiro, F. Vaz, C.J. Tavares, E. Alves, et al., Structural evolution of Ti–Al–Si–N nanocomposite coatings, *Vacuum* 83 (2009) 1206–1212.
- [19] E. Grigore, C. Ruset, X. Li, H. Dong, Zirconium carbonitride films deposited by combined magnetron sputtering and ion implantation (CMSII), *Surf. Coat. Technol.* 204 (2010) 1889–1892.
- [20] C. Oliveira, L. Gonçalves, B.G. Almeida, C.J. Tavares, S. Carvalho, F. Vaz, et al., XRD and FTIR analysis of Ti–Si–C–ON coatings for biomedical applications, *Surf. Coat. Technol.* 203 (2008) 490–494.
- [21] A.P. Serro, C. Completo, R. Colaço, F. dos Santos, C.L. da Silva, J.M.S. Cabral, et al., A comparative study of titanium nitrides, TiN, TiNbN and TiCN, as coatings for biomedical applications, *Surf. Coat. Technol.* 203 (2009) 3701–3707.
- [22] E. Silva, M. Rebelo de Figueiredo, R. Franz, R. Escobar Galindo, C. Palacio, A. Espinosa, et al., Structure–property relations in ZrCN coatings for tribological applications, *Surf. Coat. Technol.* 205 (2010) 2134–2141.
- [23] S.H.H. Yao, Y.L.L. Su, W.H.H. Kao, K.W.W. Cheng, Wear behavior of DC unbalanced magnetron sputter deposited ZrCN films, *Mater. Lett.* 59 (2005) 3230–3233.
- [24] F. Hollstein, D. Kitta, P. Louda, Investigation of low-reflective ZrCN–PVD–arc coatings for application on medical tools for minimally invasive surgery, *Surf. Coat. Technol.* 1063–1068 (2001).
- [25] M. Balaceanu, T. Petreus, V. Braic, C.N. Zaita, A. Vladescu, C.E. Cotrutz, et al., Characterization of Zr-based hard coatings for medical implant applications, *Surf. Coat. Technol.* 204 (2010) 2046–2050.
- [26] S. Calderon V., R.E. Galindo, J.C. Oliveira, A. Cavaleiro, S. Carvalho, Ag + release and corrosion behavior of zirconium carbonitride coatings with silver nanoparticles for biomedical devices, *Surf. Coat. Technol.* 222 (2013) 104–111.
- [27] W.-C. Chiang, I.-S. Tseng, P. Møller, L.R. Hilbert, T. Tolker-Nielsen, J.-K. Wu, Influence of silver additions to type 316 stainless steels on bacterial inhibition, mechanical properties, and corrosion resistance, *Mater. Chem. Phys.* 119 (2010) 123–130.
- [28] J.L. Endrino, A. Anders, J.M. Albella, J.A. Horton, T.H. Horton, P.R. Ayyalasamayajula, et al., Antibacterial efficacy of advanced silver-amorphous carbon coatings deposited using the pulsed dual cathodic arc technique, *J. Phys. Conf. Ser.* 252 (2010) 012012.
- [29] P.J. Kelly, H. Li, K.A. Whitehead, J. Verran, R.D. Arnell, I. Iordanova, A study of the antimicrobial and tribological properties of TiN/Ag nanocomposite coatings, *Surf. Coat. Technol.* 204 (2009) 1137–1140.
- [30] J.R. Morones, J.L. Elechiguerra, A. Camacho, K. Holt, J.B. Kouri, J.T. Ramirez, et al., The bactericidal effect of silver nanoparticles, *Nanotechnology* 16 (2005) 2346–2353.
- [31] J.W. Alexander, History of the medical use of silver, *Surg. Infect.* 10 (2009) 289–292.
- [32] H.J. Klases, Historical review of the use of silver in the treatment of burns. I. Early uses, 26 (2000).
- [33] I. Azócar, E. Vargas, N. Duran, A. Arrieta, E. González, J. Pavez, et al., Preparation and antibacterial properties of hybrid-zirconia films with silver nanoparticles, *Mater. Chem. Phys.* 137 (2012) 396–403.
- [34] A.D. Russell, W.B. Hugo, 7 antimicrobial activity and action of silver, *Prog. Med. Chem.* 31 (1994) 351–370.
- [35] Q.L. Feng, J. Wu, G.Q. Chen, F.Z. Cui, T.N. Kim, J.O. Kim, A mechanistic study of the antibacterial effect of silver ions on *Escherichia coli* and *Staphylococcus aureus*, *J. Biomed. Mater. Res.* 52 (2000) 662–668.
- [36] R. Kumar, H. Münsterdt, Silver ion release from antimicrobial polyamide/silver composites, *Biomaterials* 26 (2005) 2081–2088.
- [37] N.A. Trujillo, R.A. Oldinski, H. Ma, J.D. Bryers, J.D. Williams, K.C. Popat, Antibacterial effects of silver-doped hydroxyapatite thin films sputter deposited on titanium, *Mater. Sci. Eng. C* 32 (2012) 2135–2144.
- [38] P. Lalueza, M. Monzón, M. Arruebo, J. Santamaría, Bactericidal effects of different silver-containing materials, *Mater. Res. Bull.* 46 (2011) 2070–2076.
- [39] I. Carvalho, M. Henriques, J.C. Oliveira, C.F. Almeida Alves, A.P. Piedade, S. Carvalho, Influence of surface features on the adhesion of Staphylococcus epidermidis to Ag–TiCN thin films, *Sci. Technol. Adv. Mater.* 14 (2013) 035009.
- [40] V. Sambhy, M.M. MacBride, B.R. Peterson, A. Sen, Silver bromide nanoparticle/polymer composites: dual action tunable antimicrobial materials, *J. Am. Chem. Soc.* 128 (2006) 9798–9808.



- [41] J.C. Sánchez-López, M.D. Abad, I. Carvalho, R. Escobar Galindo, N. Benito, S. Ribeiro, et al., Influence of silver content on the tribomechanical behavior on Ag–TiCN bioactive coatings, *Surf. Coat. Technol.* 206 (2012) 2192–2198.
- [42] C.-H. Lai, Y.-Y. Chang, H.-L. Huang, H.-Y. Kao, Characterization and antibacterial performance of ZrCN/amorphous carbon coatings deposited on titanium implants, *Thin Solid Films* 520 (2011) 1525–1531.
- [43] G.F. Quin, Z.Y. Li, X.D. Chen, A.B. Russell, An experimental study of an NaClO generator for anti-microbial applications in the food industry, *J. Food Eng.* 54 (2002) 111–118.
- [44] S. Calderon V, R.E. Galindo, N. Benito, C. Palacio, A. Cavaleiro, S. Carvalho, Ag + release inhibition from ZrCN–Ag coatings by surface agglomeration mechanism: structural characterization, *J. Phys. D. Appl. Phys.* 46 (2013) 325303.
- [45] I. Ferreri, V. Lopes, S. Calderon V, C.J. Tavares, A. Cavaleiro, S. Carvalho, Study of the effect of the silver content on the structural and mechanical behavior of Ag–ZrCN coatings for orthopedic prostheses, *Mater. Sci. Eng., C* 42 (2014) 782–790.
- [46] C.P. Mulligan, D. Gall, CrN–Ag self-lubricating hard coatings, *Surf. Coat. Technol.* 200 (2005) 1495–1500.
- [47] M. Balaceanu, M. Braic, V. Braic, G. Pavelescu, Properties of arc plasma deposited TiCN/ZrCN superlattice coatings, *Surf. Coat. Technol.* 200 (2005) 1084–1087.
- [48] S.C. Velasco, V. Lopez, C.F.A. Alves, A. Cavaleiro, S. Carvalho, Structural and electrochemical characterization of Zr–C–N–Ag coatings deposited by DC dual magnetron sputtering, *Corros. Sci.* 80 (2014) 229–236.
- [49] C. Palacio, C. Gómez-Aleixandre, D. Díaz, M. García, Carbon nitride thin films formation implantation by Ni ion, *Vacuum* 48 (1997) 709–713.
- [50] C. Huang, Z. Tang, Z. Zhang, Differences between zirconium hydroxide ( $Zr(OH)_4 \cdot nH_2O$ ) and hydrous zirconia ( $ZrO_2 \cdot nH_2O$ ), *J. Am. Ceram. Soc.* 84 (2004) 1637–1638.
- [51] A. Siozios, H. Zoubos, N. Pliatsikas, D.C. Koutsogeorgis, G. Vourlias, E. Pavlidou, et al., Growth and annealing strategies to control the microstructure of AlN:Ag nanocomposite films for plasmonic applications, *Surf. Coat. Technol.* 255 (2014) 28–36.
- [52] M.S. Bootharaju, G.K. Deepesh, T. Pradeep, Atomically precise silver clusters for efficient chlorocarbon degradation, *J. Mater. Chem. A* 1 (2013) 611–620.
- [53] C.-N. Lok, C.-M. Ho, R. Chen, Q.-Y. He, W.-Y. Yu, H. Sun, et al., Silver nanoparticles: partial oxidation and antibacterial activities, *J. Biol. Inorg. Chem.* 12 (2007) 527–534.
- [54] A. Taglietti, C.R. Arciola, A. D'Agostino, G. Dacarro, L. Montanaro, D. Campoccia, et al., Antibiofilm activity of a monolayer of silver nanoparticles anchored to an aminosilanized glass surface, *Biomaterials* (2013) 1–10.
- [55] J.C. Kotz, P.M. Treichel, J.R. Townsend, *Chemistry and chemical reactivity*, Books/Cole Cengage Learning 8th edition, 2011.
- [56] D. Hecht, H.-H. Strehblow, XPS investigations of the electrochemical double layer on silver in alkaline chloride solutions, *J. Electroanal. Chem.* 440 (1997) 211–217.
- [57] M. Rajcic-Vujasinovic, V. Grekulovic, Z. Stevic, N. Vukovic, Potentiostatic oxidation of AgCu50 alloy in alkaline solution in the presence of chlorides, *Corros. Sci.* 70 (2013) 221–228.